Rate Independent Simulation of Shear Localization in Channel Die Compression

Awni Abu-Saman

Department of Math., Faculty of Scienc
Al-Azhar University-Gaza, Gaza-Palestine.
Email: awni_saman@yahoo.com

ملخص: هذا البحث يصف التشوه البلاستيكي الكبير الناتج عن ضغط بلورة نحاسية بقوة . مفهوم التشوه البلاستيكي الذي لا يعتمد على الزمن في البلورات الأحادية أُستخدم مع مفهـوم " الـسطح الإضافي" لدراسة الانزلاق المتراكم أثناء التشوه البلاستيكي الكبير للمادة.

التطبيق العددي تم باستخدام خوارزمية رياضية جديدة لبرنامج اباكوس Abaqus وقد تبين مـن خلال النتائج كفاءة الخوارزمية المستخدمة وتطابق النتائج مع النتائج العملية والنظرية.

Abstract: *This work describes the large plastic deformation and shear localization in channel die compression of a single copper crystal. The rate independent deformations in single crystals with the concept of "extremal surface" is used. The numerical implementation involved the use of a user material subroutine UMAT in FE program ABAQUS to evaluate large deformations. Numerical simulations are presented that illustrate the excellent performance of the algorithm. Good agreement was found with rate dependent computations.*

Keywords: Single crystals, Constitutive behavior, Finite elements.

INTRODUCTION

It is well known that phenomena responsible for inelastic deformation are usually very complicated. As a result models of plasticity end gradually towards describing more and more elementary processes. In order to describe in more detail plasticity based on slips, the crystal plasticity has been introduced by Peirce et al. [18], Asaro[3], Kalidindi [10], Kirchner[11], Abu-Saman [1]. In the last years we observe a development of methods of modeling applied to plasticity Zbib & Rubia [20], Gearing et al. [9], such methods also reflect a tendency to considering the most elementary effects responsible for plastic deformation. Deve & Asaro [5] stated that, in large plastic deformation of polycrystalline materials, shear bands play an important part in the deformation process and shear localization

progressively replaces the current deformation process by slipping and/or twinning. This change in deformation mode contributes to the development of strain induced anistropy and modifies remarkably material properties.

The attempt to formulate a simple phenomenological model of large plastic deformations accounting for shear bands on the macroscopic level seems to be important for adequate theoretical description of inelastic behavior of metallic solids. Physical nature of shear banding is not yet completely explained. In particular, mechanisms of initiation and propagation of micro-shear bands across grain boundaries is a little known process. According to studies reported by Kusnierz [13] this happens after reaching certain critical point on the loading or deformation path, represented by the critical value of flow stress or equivalent strain. In Korbel [12] the active micro shear bands appear as a kind of self-induced deformation modes.

Pecherski's [16,17] theoretical studies on the basic physical mechanisms of micro-shear banding lead to a formulation of a phenomenological model of plastic flow accounting for micro-shear bands, and model the effect of micro-shear bands. He used the Huber-Mises yield criterion to approximate the extremal surface. A double-shearing system, normal to the flow plane, is used to represent contribution of active micro-shear bands. Pecherski [16] proposed the net fraction parameter to approximate the contribution of the shear bands in the plastic deformation process, and a crystalline parameter to approximate the mean orientation of micro-shear bands.

This paper contains Finite Element computations of large plastic deformation and shear localization of single crystals. A numerical algorithm by Abu-Saman [2] is developed as a user material subroutine UMAT in FE program ABAQUS for evaluation of equivalent plastic strains.

BASIC NOTATIONS

The following notations are employed: **s** represents the deviatric stress, and **e** is the deviatoric strain. These tensors are defined by

$$\mathbf{s} = \sigma - \frac{1}{3}(\mathrm{tr}\sigma)\mathbf{1},$$

$$\mathbf{e} = \varepsilon - \frac{1}{3}(\mathrm{tr}\varepsilon)\mathbf{1},$$

where **1** is the second order unit tensor and $\mathrm{tr}\sigma$, $\mathrm{tr}\varepsilon$ are traces of stress and strain tensors.

The natural inner products of the linear vector spaces of deviatoric stress and deviatoric strain are defined as

$$\mathbf{s} : \bar{\mathbf{s}} = \mathrm{tr}[\mathbf{s} \,.\, \bar{\mathbf{s}}^{t}] \equiv s_{ij}\, \bar{s}_{ij} \,,$$

$\mathbf{e} : \bar{\mathbf{e}} = \mathrm{tr}[e . \bar{e}^{t}] \equiv e_{ij} \bar{e}_{ij}$,

where $(.)^{t}$ is the transposed operator. The norms associated with these inner products are defined as follows

$\|\mathbf{s}\| = [\, \mathbf{s} : \mathbf{s} \,]^{1/2} = \sqrt{2\, J_2(\mathbf{s})}$

$\|\mathbf{e}\| = [\mathbf{e} : \mathbf{e}\,]^{1/2} = \sqrt{2\, J_2(\mathbf{e})}$

where $J_2(\mathbf{s})$ and $J_2(\mathbf{e})$ are the second invariants of the stress and strain tensors.

BASIC CONSTITUTIVE EQUATIONS

The extremal surface is approximated by Huber-Mises yield criterion Mises [15], which is used in the model of small distortional elastic strains and finite plastic deformations. The extremal surface is defined by the equation

$$f(\mathbf{S},k) = \|\mathbf{S}\| - \sqrt{2}\ \kappa(\gamma_{eq}) = 0\,, \qquad \gamma_{eq} = \int_0^t \dot{\gamma}_{eq}\, dt \tag{1}$$

$$\dot{\gamma}_{eq} = (2\mathbf{D}^{P} : \mathbf{D}^{P})^{1/2} = \sqrt{2}\|\mathbf{D}^{P}\| \tag{2}$$

where **S** is the deviator of Kirchhoff stress, γ_{eq} and $\dot{\gamma}_{eq}$ are the shear strain and the shear strain rate respectively, and κ is hardening rule.

The *J2* flow theory is assumed for the case when the sole mechanism of crystallographic multiple slip is responsible for plastic deformation. The contribution of mechanisms of crystallographic multiple slip is approximated by the flow rule

$$\mathbf{D}_S^{P} = \frac{\sqrt{2}}{2}\dot{\gamma}_{eq}\, \hat{\mathbf{N}}, \tag{3}$$

$$\dot{\gamma}_{eq} = \sqrt{2}\,[\,\eta\,], \tag{4}$$

where $\hat{\mathbf{N}} = \frac{\mathbf{s}}{\|\mathbf{s}\|}$, $\mathbf{D}_S^{P}$ is the plastic deformation rate, $\dot{\gamma}_{eq}$ is the shear rate when crystallographic multiple slip is the sole mechanism for plastic deformation, $\hat{\mathbf{N}}$ is the unit vector normal to the surface defined by (1). Let **D** represents the total deformation rate expressed by

$$\mathbf{D} = \mathbf{D}^{e} + \mathbf{D}_S^{P}\ , \tag{5}$$

$$\mathbf{D} = (\mathbf{L}^{-1} + \frac{\alpha}{2h}\hat{\mathbf{N}} \otimes \hat{\mathbf{N}}) : \tau^{\circ}\,, \tag{6}$$

where $h = \frac{\partial\, \kappa}{\partial\, \gamma_{eq}}$ is the plastic hardening modulus, τ° is the structure corotational objective rate of the Kirchhoff stress , **L** is the elastic modulus,

$$\eta = \frac{\tau^{\circ} : \hat{\mathbf{N}}}{2h}$$

$[\eta] = \eta; \alpha = 1$ *if* $\eta > 0$ *and* f = 0,

$[\eta] = \eta; \alpha = 0$ *if* $\eta \le 0$ *or* f < 0.

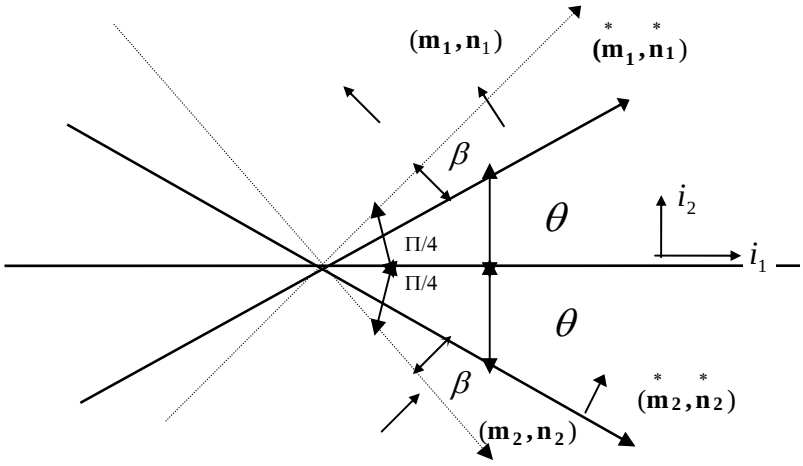

Figure (1): Geometry shows the double shear system in the extremal surface model

Following Pecherski [16], a double-shearing system normal to a flow plane is used to represent a contribution of active micro-shear bands. Directions $(\overset{*}{\mathbf{m}}_i, \overset{*}{\mathbf{n}}_i)$, i =1,2, of the double-shearing system represent the shear direction $\overset{*}{\mathbf{m}}_i$ while $\overset{*}{\mathbf{n}}_i$ is normal to a shear direction. The angle θ in Fig. 1 approximates the mean orientation of micro-shear bands and it is a crystalline parameter for a single crystal which is statistically averaged for a polycrystalline aggregate. The compression direction is i_1.

The unit vectors $(\overset{*}{\mathbf{m}}_i, \overset{*}{\mathbf{n}}_i)$, i =1,2, are obtained directly from geometrical relations in Fig. 1 and can be written in terms of angle β and unit vectors $(\mathbf{m}_i, \mathbf{n}_i)$, i = 1,2, where β is the angle of rotation of planes of active micro-shear bands relative to planes of maximum shear stress. From Fig. 1 $\beta = \frac{\pi}{4} - \theta, \ \theta \in (0, \frac{\pi}{2})$ where θ is regarded as a crystal parameter which approximates the mean orientation of micro-shear bands.

The rate of plastic deformations and plastic spin produced by active

micro-shear bands is given by

$$\mathbf{D}^{\mathrm{p}}_{\mathrm{mb}} = \sum_{i=1}^{2} \overset{\bullet}{\gamma}{}^{i}_{\mathrm{mb}} (\overset{*}{\mathbf{m}}_i \otimes \overset{*}{\mathbf{n}}_i)_s \,, \tag{7}$$

where $\overset{\bullet}{\gamma}{}^{\mathrm{i}}_{\mathrm{mb}}$ is the rate of plastic shearing along the i-th direction of shear. According to Fig.1, equation (7) can be re-written as:

$$\mathbf{D}^{\mathrm{p}}_{\mathrm{mb}} = \frac{\sqrt{2}}{2}\cos 2\beta (\overset{\bullet}{\gamma}{}^{1}_{\mathrm{mb}} - \overset{\bullet}{\gamma}{}^{2}_{\mathrm{mb}})(\mathbf{m}_1 \otimes \mathbf{n}_1) + \frac{1}{2}\sin 2\beta \; (\sum_{i=1}^{2} \overset{\bullet}{\gamma}{}^{\mathrm{i}}_{\mathrm{mb}})(\mathbf{m}_1 \otimes \mathbf{m}_1 - \mathbf{n}_1 \otimes \mathbf{n}_1)$$

The rate of plastic deformation can be expressed as an additive decomposition of two rates: one caused by mechanisms of crystallographic slip $\mathbf{D}^{\mathrm{P}}_{\mathrm{S}}$, and the second occurring due to existence of micro-shear bands $\mathbf{D}^{\mathrm{p}}_{\mathrm{mb}}$,

$$\mathbf{D}^{\mathrm{p}} = \mathbf{D}^{\mathrm{P}}_{\mathrm{S}} + \mathbf{D}^{\mathrm{p}}_{\mathrm{mb}} \,, \tag{8}$$

$$\overset{*\bullet}{\gamma} = \gamma^{\bullet}_{\mathrm{eq}} + \gamma^{\bullet}_{\mathrm{mb}} \,, \tag{9}$$

where $\overset{*\bullet}{\gamma}$ is the total plastic shearing rate, $\gamma^{\bullet}_{\mathrm{eq}}$ is the shear rate from the crystallographic slip mechanism, and $\gamma^{\bullet}_{\mathrm{mb}}$ is the rate of plastic shearing produced by micro-shear bands.

The unit normal vector to the yield surface $\hat{\mathbf{N}}$ and the unit orthogonal vector to it $\hat{\mathbf{T}}$ can be written in terms of double shearing directions (e.g., Pecherski [16]).

$$\hat{\mathbf{N}} = \sqrt{2}\,(\mathbf{m}_1 \otimes \mathbf{n}_1)\,, \tag{10}$$

$$\hat{\mathbf{T}} = \frac{\sqrt{2}}{2}(\mathbf{m}_1 \otimes \mathbf{m}_1 - \mathbf{n}_1 \otimes \mathbf{n}_1)\,. \tag{11}$$

From the consistency condition $\overset{\bullet}{f}(\mathbf{S},k) = 0$, the total shearing rate can be written as

$$\overset{\bullet}{\gamma}{}^{*} = \frac{\sqrt{2}}{2\mathrm{h}}(\tau^{\circ} : \hat{\mathbf{N}})\,. \tag{12}$$

The orthogonal component $\hat{\mathbf{T}}$ can be written in terms of the deviator Kirchhoff stress $\tau^{\circ\bullet}$ as:

$$\hat{\mathbf{T}} = \Lambda\,[\tau^{\circ\bullet} - (\tau^{\circ} : \hat{\mathbf{N}})\hat{\mathbf{N}}]\,. \tag{13}$$

where $\Lambda = \left\| \tau^{\circ\bullet} - (\tau^{\circ} : \hat{\mathbf{N}})\hat{\mathbf{N}} \right\|^{-1}$ is the normalizing factor.

Following Pecherski [16], the rate of plastic deformation $\mathbf{D}^{\mathrm{P}}$ can be written in terms of active micro-shear fractions $\mathrm{f}^{(1)}_{\mathrm{ms}}$ and $\mathrm{f}^{(2)}_{\mathrm{ms}}$

$$\mathbf{D}^{P} = \frac{1}{2h}(\tau^{\circ}:\hat{\mathbf{N}})\hat{\mathbf{N}} + \frac{\Lambda}{2h}(\tau^{\circ}:\hat{\mathbf{N}})(f_{ms}^{(1)} - f_{ms}^{(2)})\tan 2\beta\ [\tau^{\circ\bullet} - (\tau^{\circ}:\hat{\mathbf{N}})\hat{\mathbf{N}}], \qquad (14)$$

by substitution (12) and (13) into (14), $\mathbf{D}^{P}$ can be written in terms of $\hat{\mathbf{T}}$ and $\hat{\mathbf{N}}$

$$\mathbf{D}^{P} = \frac{\gamma^{\bullet *}}{\sqrt{2}}[\hat{\mathbf{N}} + \hat{\mathbf{T}}(f_{ms}^{(1)} - f_{ms}^{(2)})\tan 2\beta\ ]. \qquad (15)$$

NUMERICAL RESULTS

The numerical analysis is conducted by using the finite element program ABAQUS with constitutive relations incorporated into a user subroutine. The user material subroutine algorithm used is developed by Abu-Saman [2]. The deformation is modeled by considering a small part of a crystal as a representative unit volume. Actual dimensions of a region are irrelevant to this model, since constitutive relations do not include a size scale. The initial height and width of a model region are $L_{\circ} = 1.5\ W_{\circ}$ and $S_{\circ} = W_{\circ}$, $S_{\circ}$ is the out-of plane dimension (Fig. 3).

Compression is along the y direction. The material extends in the x direction and z is the out of plane direction.

The crystal is represented by five hundred and seventy square, two-dimensional, plane-strain, four-nodded elements. The finite element mesh consists of 30 quadrilaterals in the y-direction and 19 in the x-direction. The boundary conditions are the following:

$U_y = 0$ along $y = 0$

$U_y = -.001 L_{\circ}$ along $y = L_{\circ}$

$U_x = 0$ along $x = 0$

$U_x =$ constant along $x = W_{\circ}$

All surfaces are constrained to remain planar. The boundary conditions are shown in Fig.(4). The elastic constants used in the finite element calculations are C_{11}=842.0 $\tau_{\circ}$, C_{12}= 607.0 $\tau_{\circ}$ and C_{44}=377.0 $\tau_{\circ}$, that correspond to Young's modulus E=1000 $\tau_{\circ}$, where $\tau_{\circ}$ is the yield limit, and Poisson's ratio υ=0.3. The constants are taken to fit the elastic anisotropy of a copper single crystal [7]. The net fraction is given by

$F_{ms}^{net} = \frac{A}{(1+e^{B-c|\varepsilon|})}$, where A=0.9, B=6.5, C=11.8, and $\beta = 0.5^{\circ}$.

The hardening law is defined by:

$$\kappa = \tau_\circ + \frac{8.9\tau_\circ}{11.125}\tanh(11.125\gamma).$$

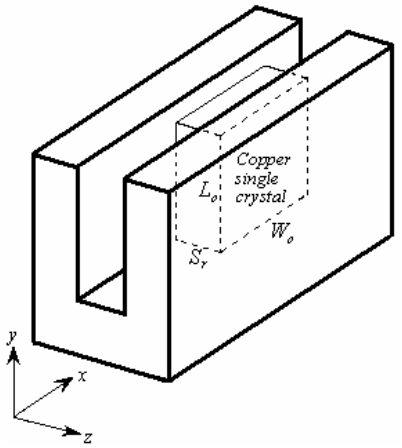

Figure 3 A copper single crystal in a channel die

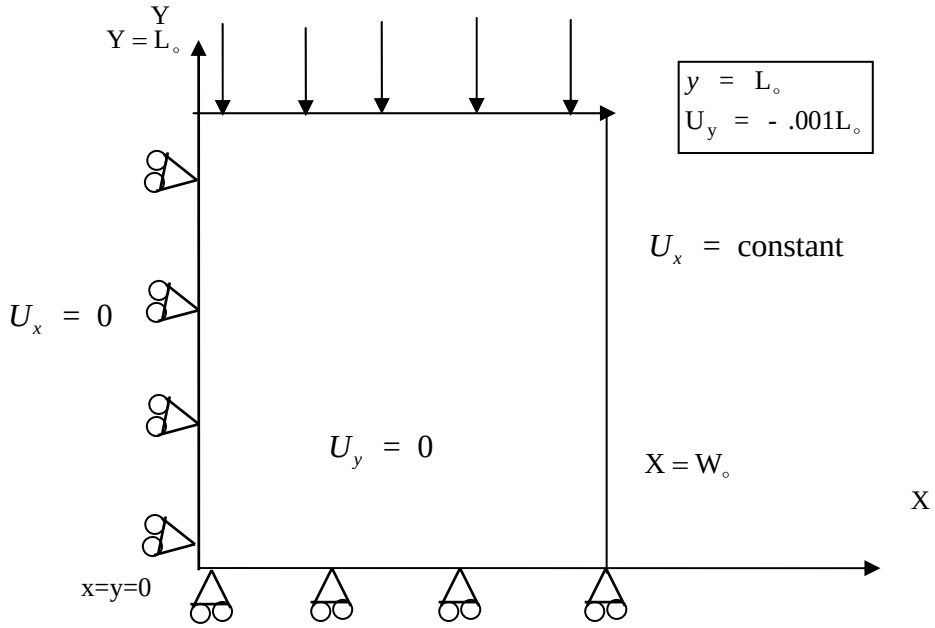

Figure(4): Boundary conditions applied to the copper crystal deformed in a channel die.

Deformed finite element meshes for the plain strain compression simulation are shown in Figs.(5(a)-5(c)) for various values of the compressive logarithmic strain $\varepsilon_{22} = -\ln(L/L_\circ)$ with the current L and the initial length $L_\circ$ of the finite element mesh along y-direction. In Fig. 5(c) a shear band formation is clear.

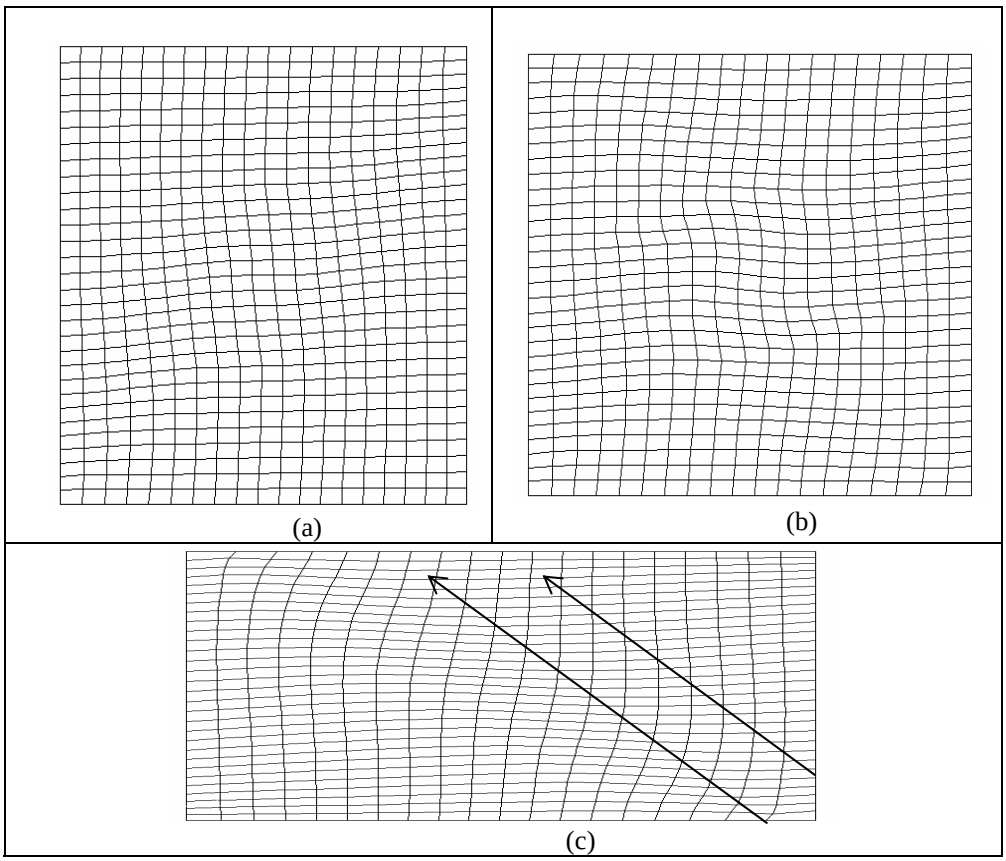

Figure (5): Deformed finite element meshes for a copper single crystal, for various values of strain (a) ε_{22} =0.164, (b) ε_{22} =0.255, (c) ε_{22} =0.58.

Figs.(6-8) show the corresponding strain levels depicted in Fig.(5). Fig.(6(a)) and (6(b)) show that the deformation is becoming non-uniform. When ε_{22} = 0.164 the shear localized in a zone from north-east to the south-west, with the highest slip rate in localized zone, but strains do not exceed the applied uniform strain of 0.164. Fig.(7) corresponding to strain level depicted in Fig.(5(b)) shows the start of localization in the zone from the north-west to the south-east. Fig.(8), that corresponds to strain level depicted in Fig.(5(c)) shows the propagation of shear mode in a form of a shear band across the north-west to the south-east of the specimen inclined at an angle approximately equal to 36° to the horizontal direction. The angle of inclination is consistent with computational results of (bcc) crystal rate dependent simulations carried by Peirce et al. [18], Abu-Saman [1] and experimental results conducted by Chang & Asaro [4] on single crystals.

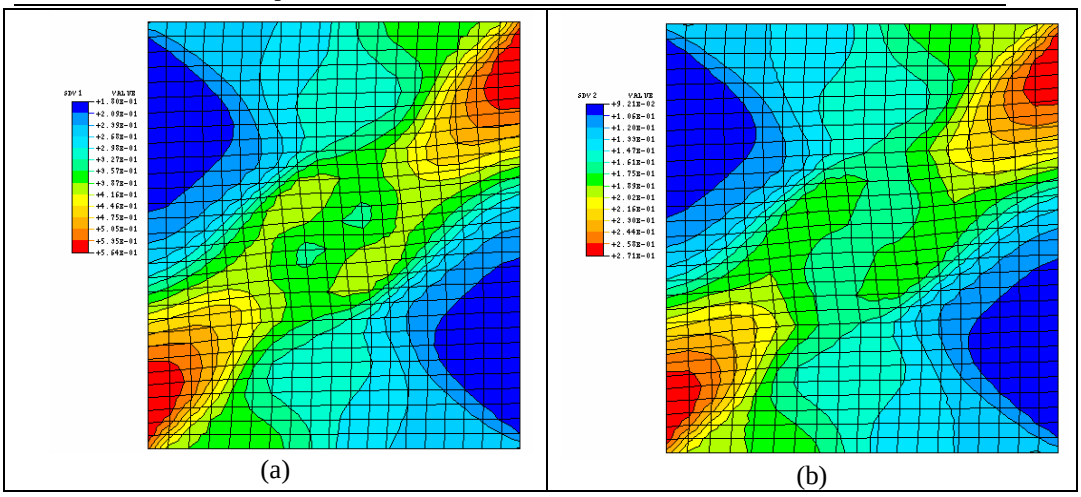

(a) (b)

Figure(6): (a)contours of accumulated slip; (b) contours of equivalent strain; for the strain ε_{22} =0.164 for a deformed copper crystal shown in Fig.5(a).

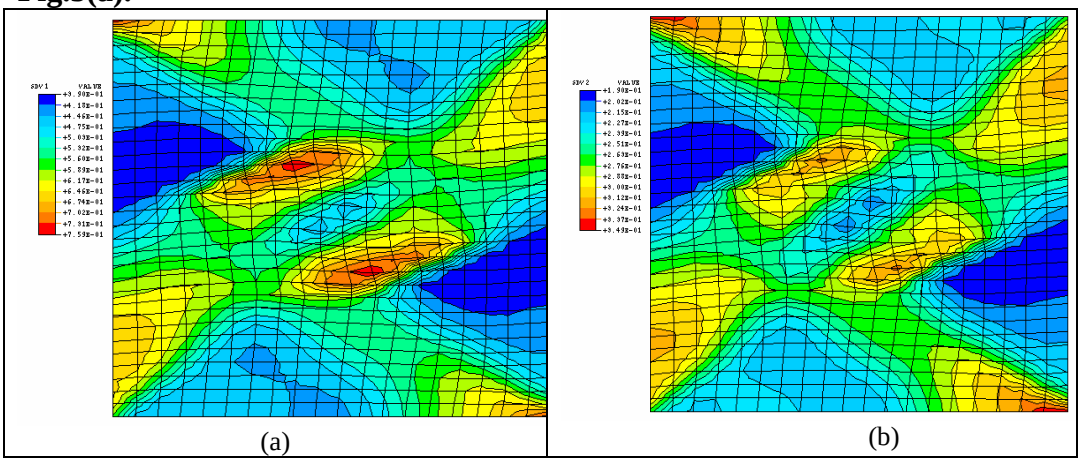

(a) (b)

Fig.(7): (a)Contours of accumulated slip; (b)contours of equivalent strain for strain ε_{22} =0.255 for a deformed copper crystal shown in Fig. 5(b).

Strain inside the shear band reached a value of 1.17, which is significantly higher than the applied strain of 0.58. This agrees with Harren et al. [6] plane strain compression results. It is noticeable that the shear band in Fig.(5(c)) is not sharp and the shear localization zone is wide.

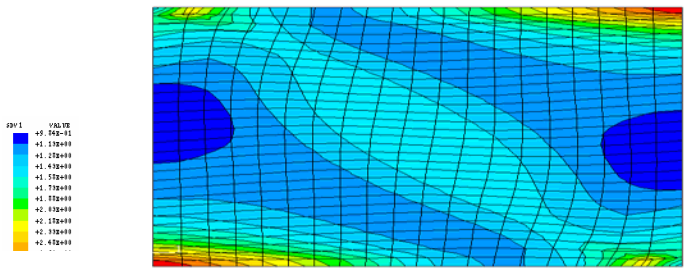

(a)

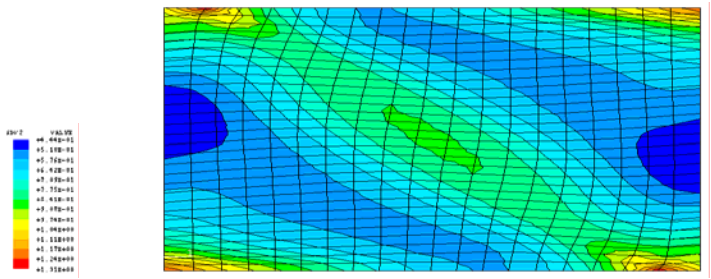

(b)

Figure(8): (a) Contours of accumulated slip; (b) contours of equivalent strain for the strain ε_{22} = 0.58 for a deformed copper crystal shown in Fig. 5(c).

CONCLUSIONS

In this paper the rate independent constitutive equations have been formulated and implemented to study shear localization in single crystals. These constitutive equations are a natural, more physical generalization of the classical J_2 rate independent flow theory, and the integration procedure is a generalization of the classical return mapping algorithm. The algorithm was successfully implemented into ABAQUS using the user material subroutine UMAT. The ABAQUS modeling results of shear bands in a channel die problem showed good agreement with the experimental and numerical computational results. In the simulation of the copper single crystal, the angles of inclination of shear bands and the onset of non-uniform localization agree with experimental results obtained by Embury et al. [8] and Harren et al. [6] for (bcc) crystals, and with the rate dependent numerical computations carried out by Peirce et al. [18] and Abu-Saman [1]. In spite of the complexity, the extremal surface concept of large plastic deformation can be applicable in modeling of large plastic deformations under highly constrained conditions.

Acknowledgments **-** I would like to thank Jacek Ronda (D.Sc.) for his comments and suggestions during this research. I would like gratefully to acknowledge a support provided from the FRD/UCT Center for Research in Computational and Applied Mechanics (CERECAM) in South Africa for making the computational facilities available.

REFERENCES

1. Abu-Saman, A. M., *Journal of Rajasthan Academy of Physical Science* **2003**, 2, 1.
2. Abu-Saman, A. M., *Journal of Rajasthan Academy of Physical Sciences* **2002**,1,1.
3. Asaro, R. J., *J. App. Mech.* **1983**, 50, 921.
4. Chang, Y. W. and Asaro, J., *Acta. Metal.* **1981**, 29, 241.
5. Deve, H. E. and Asaro, R. J., *Metall. Trance*, 20A **1989**, 590.
6. Harren, S. V., Deve, H. E. and Asaro, R. J., *Acta Metal.* **1988**, 36, 2435
7. Hughes, T. and Winget, J., *Intl. J. for Numerical Methods in Eng.* **1980**, 15, 1862.
8. Embury, J. D., Korbel, A., Raghunathan V.S. and Rys, J, *Acta Metal.* **1984**, 32, 1883.
9. Gearing, B. P., Moon, H. S., Anand, L, *Int. J. of Plasticity* **2001**,17, 23.
10. Kalidindi, S. R., *Int. J. of Plasticity* **2001**, 17, 837.
11. Kirchner, E., *Int. J. of Plasticity* **2001**, 17, 907.
12. Korbel, A., *In proc. Intl. Symposium on Plastic Instability, Presses de l` Ecole nationale des ponts et chausees , Paris* **1985**, 325.
13. Kusnierz, J., *Arch. Metall.* **1992**, 37, 203.
14. L.P.Kubin, L. P. and Devincre, *(20th Risoe symposium), J. B. Blide Soerensen et al. (Eds.), Risoe natl. lab., Roskilde, Denmark,* **1999** *pp.* 61-83, 1999.
15. Mises R. V., *Mathematik and Mechanik* **1928**, 8, 161.
16. Pecherski, R. B., *Arch. Mech* **1992(a)**, 44, 563.
17. Pecherski, R. B., *ZAMM, 72* **1992(b)** *pp*. T250-T254.
18. Peirce, D., Asaro, R. J. and Needleman, A., *Acta. Metal.* **1983**, 31, 1951.

19. Simo, J. C., *Computer Methods in Applied Mechanics and Engineering* **1988**, 68, 1.

20. Zbib, H. M. and Rubia, H. M, *Int. J. of Plasticity*, **2002**, 18, 1133.